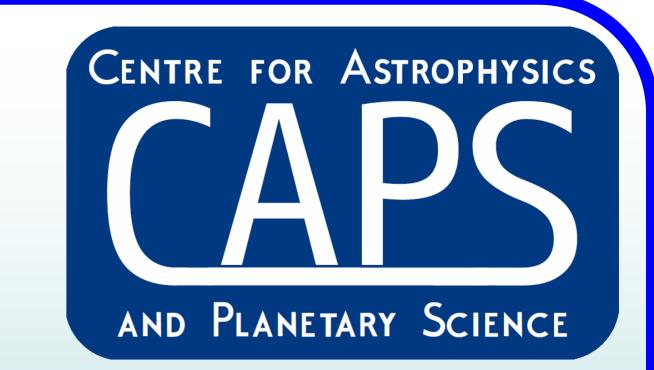


RESULTS FROM RAMAN ANALYSES OF THIRTY-SIX STARDUST COMETARY GRAINS FROM TRACKS 170, 176, 177, 178



M. C. Price¹, J. C. Bridges², P. J. Wozniakiewicz^{1,3} and L. J. Hicks²

¹School of Physical Sciences, University of Kent, Canterbury, Kent, CT2 7NH, UK (mcp2@star.kent.ac.uk).

²Space Research Centre, Dept. of Physics & Astronomy, University of Leicester, LE1 7RH, UK. ³Earth Sciences Department, Natural History Museum, Cromwell Road, London, SW7 5BD, UK.

Introduction

We present Raman spectroscopy results from a set of terminal grains found in tracks C2112,4,170,0,0 ('170', 1 grain), C2045,2,176,0,0 ('176', 10 grains), C2045,3,177,0,0 ('177, 12 grains') and C2045,4,178,0,0 ('178', 13 grains) taken from the cometary side of NASA's Stardust mission sample collector [1]. In order to maximise the scientific return, it is vital that analyses of the samples are undertaken using as many different, non-destructive, techniques as possible preferably on particles whilst they are still embedded in aerogel using, for example, Raman spectroscopy [2] and XRD [3]. We used a Labram-HR Raman spectrometer at Kent to study the terminal grains. This spectrometer incorporates four lasers: 785 nm, 633 nm, 532 nm and 473 nm. The maximum 473 nm laser power at the sample is 30 mW, but here, a 10% neutral density filter was used at all times which limited the power at the sample (through a ×50 objective) to a maximum of ~3 mW, thus avoiding unwanted heating and possible modification of the grain [4]. Upon receipt, the keystones were carefully unwrapped and photographed. Track 170 was mounted on a glass slide covered with kapton tape which proved to be highly fluorescent, thus necessitating the use of the 633 nm wavelength laser to obtain any Raman signal. Tracks 176, 177 and 178 were mounted between thin (thickness unknown) silicon nitride windows, which greatly reduced fluorescence permitting a 473 nm excitation wavelength to be used on these grains.

TABLE 1: Results from Track 176 (see text).					
Grain ID	X, Y, Z (μm)	Composition Carbon (weak), enstatite, aerogel			
TG #1	(0,0,0)				
TG #2	(-14.1,-52.5,-63.3)	Enstatite, aerogel (weak)			
SG 'a'	(-37.5,+56.3,-5.8)	Olivine (>Fo ₅₀), carbon (strong)			
SG 'b'	(-35.2,+142.6,-11.9)	Olivine (>Fo ₆₀), enstatite (?), aerogel			
SG 'c'	(-43.6,+171.6,-15.4)	Aerogel, unknown line at 227 cm ⁻¹			
SG 'd'	(-15.4,+175.9,-38.2)	Carbon (weak), aero- gel			
SG 'e'	(-11.8,+203.5,+9.8)	Carbon, enstatite, (strong) aerogel			
SG 'f'	(-8.1,+206.4,+4.8)	Carbon (?), aerogel			
SG 'g'	(-51.1,+209.8,-25.4)	Carbon (strong), aerogel, unknown at 2325 cm ⁻¹)			
SG 'h'	(-25.4,+262.8,-7.0)	Carbon (?), aerogel			

TARLE 2: Results from Track 177 (see text)

Grain ID	X, Y, Z (μm)	Composition	
TG #1	(0,0,0)	Olivine (>Fo ₈₀),Carbon, aerogel	
TG #2	(-5.9,+1.4,+8.8)	Unknown lines at (214.8, 279.1 cm ⁻¹)	
SG '2'	(+85.3,+187.5,-45.5)	No definite lines (grain moved)	
SG '3'	(+62.6,+205.7,+50.7)	Olivine (>Fo ₈₀),Carbon (strong), aerogel	
SG '4'	(+22.1,+172.9,-3.1)	Carbon, aerogel	
SG '5' \TG#1A	(-14.3,+13.2+34.9)	Unknown (weak) lines at ~250 cm ⁻¹	
SG '6'	(+43.4,+364.7,-44.8)	No definite lines	
SG '7'	(+24.5,+435.0,-5.8)	Carbon	
SG '8'	(+17.4,+461.4,-0.1)	Carbon	
SG '9'	(+20.1,+461.4,-0.1)	Carbon (strong)	
SG '10'	(+45.2,+459.8,-0.6)	Carbon (strong)	
SG '11'	(+53.7,+462.8,-0.8)	Carbon (weak)	
	I	1	

Grain ID	X, Y, Z (μm)	Composition	Grain ID	X, Y, Z (μm)	Composition
TG #1	(+753.5,-729.0,+5.4)	Olivine (>Fo ₈₀), Carbon, aerogel	SG '5'	(-47.0,+966.6.+12.6)	Aerogel
TG #1b	(+780.0,-636.9,-18.2)	Olivine (>Fo ₈₀)	SG '6'	(-14.1,+999.1,+10.8)	Carbon (v. strong)
TG #1c	(+5.7,+99.4,-0.4)	Carbon, enstatite	SG '7'	(-22.8,+1098.3,+4.8)	Olivine (>Fo ₆₀), Carbon
SG '2'	(+802.4,-195.5,-3.0)	Olivine (>Fo ₈₀)	SG '8'	(-17.5,+1170.0,-6.1)	Olivine (>Fo ₈₀), Carbon
SG '3'	(+728.6,+19.1,+30.5)	Olivine (>Fo ₈₅)	SG '9'	(-29.6,+1193.2,-9.5)	Olivine (>Fo ₈₀), Carbon (strong)
SG '4'	(+48.6,+949.5,-28.7)	Aerogel	SG '10'	(-34.9,+1208.4,-16.4)	Olivine (>Fo ₈₀), Carbon (strong)

Results

<u>Track 170:</u> Previous in situ XANES and EXAFS analyses carried out on the terminal grain of track 170 concluded that the grain contained a mixture of Fe-metal and Cr- and Ca-bearing silicate [5]. Raman spectroscopy results supported the initial results of Bridges *et al*, and determined that the mineralogy of the silicate phase was Mg-rich olivine, Fo_{95} [6], after correcting for changes in mineralogy due to impact heating [7, 8].

<u>Tracks 176, 177, 178:</u> Tables 1, 2 and 3 gives the ID ('TG' = Terminal Grain, 'SG' = subgrain) and the position of the subgrains relative to the largest terminal particle. The right hand sketch in Fig. 1 gives the orientation of the co-ordinate system used to mark the position of the subgrains relative to the terminal grain position. The detected composition of the grains are also given as well as contaminating aerogel (if detected).

<u>Comparison to chondrules:</u> In order to provide a comparison with the <u>Stardust</u> organic analyses, a sample of CR3 chondrite QUE 99177 was analysed (kindly supplied by A. Brearley). This sample is rich in carbon globules and has undergone minimal aqueous alteration [9]. Initial Raman mapping has been undertaken on four of the chondrules and the preliminary results indicates that they are mostly olivine in composition, but with a mix of haematite. One grain is particularly carbon-rich. Analysis is still ongoing, and will be presented in due course. The full set of results for all four of the <u>Stardust</u> grains presented here will be submitted to <u>MAPS</u> in Summer 2014.

Conclusions & References

- 1. Track #176 presents significant carbon signatures with strong olivine and enstatite (verified in [3]).
- 2. Track #177 is olivine rich (Mg rich olivines) with some carbon (verified in [3]).
- 3. Track #178 has significant carbon (especially around the bulb), but fewer olivine signatures. Could be a reflection of the bulb-like nature of the track, implying an organic rich impactor, with embedded magnetite grains (forming much of the terminal particles, [3]).
- 4. Track #170's terminal grain gives a weak olivine (Fo_{95}) signature, but the position of the Fe K absorption edge, and pre-edge centroid, are consistent with Fe in the terminal grain being pre-dominantly metallic.
- 5. There are potentially hundreds of micron-sized (and smaller) subgrains the *Stardust* tracks than just the terminal particles.
- 6. Subgrains have different compositions to the larger terminal particles.
- 7. Carbonaceous material seems to be concentrated around the bulb(s), possibly indicative of the (organic?) 'glue' that held the aggregate impactor together.
- 8. Laser heating is a potential problem [10], and care has to be taken. A temperature calibration for olivine (and other minerals) is needed using Stokes/Anti-Stokes line ratios.

[1] Brownlee D. E. et al. (2006), *Science*, 314, 1711. [2] Wopenka B. (2012), *MAPS*, 47.4, 565. [3] Hicks L. et al. (2014). *45th LPSC*, #2051. [4] de Faria D. L. A et al. (1997). *J. Raman Spec.*, 28, 873. [5] Bridges J. C. et al (2012), *43rd LPSC*, abstract #2214. [6] Price M. C et al (2012), *EPSC*, EPSC2012-333. [7] Burchell M. J. et al., (2006). *MAPS*, 41.2, 217. [8] Foster N. J. et al. (2012). *GCA*, 121, 1. [9] Abreu N. et al (2008). 39th LPSC, #2013. [10] Hibbert R. et al. (2014). *45th LPSC* #1350.

Fig. 1: Images of tracks 176, 177, 178 showing the position of the main terminal grains. The right hand sketch gives the co-ordinate system used to record the position of the sub-grains.

